Electronic Supplementary Information for

"Deep-Learning-Enhanced Modeling of Electrosprayed Particle Assembly on Non-spherical Droplet Surfaces"

Nasir Amiri[a], Joseph M. Prisaznuk[b], Peter Huang[b], Paul R. Chiarot[b†], Xin Yong[a*]

[a] Department of Mechanical and Aerospace Engineering, University at Buffalo, Buffalo, NY 14260, USA

[b] Department of Mechanical Engineering, Binghamton University, Binghamton, NY 13902, USA

Supplementary Tables

Table S1. Mesh dependency test

	Coarse	**Fine**	**Finer**
Maximum element size in air near droplet (mm)	2.22	0.112	0.0575
Max element size inside droplet (mm)	0.64	0.115	0.0526
Number of tetrahedral elements (millions)	0.0292	0.32	1.915
Average voltage at the droplet surface	0.185544	0.131559	0.130557
Variation of voltage with respect to 'finer' (%)	42.12	0.7674	0
Average voltage (w/o contact line) at the droplet surface	0.110914	0.090545	0.090406
Variation of voltage (w/o contact line) with respect to 'finer' (%)	22.68	0.1541	0

Table S2. Best hyperparameter configuration from Ray Tune

Hyperparameters	**Value**
Number of layers	5
Number of neurons in each layer	448
Maximum iterations	646
Initial learning rate	0.0279
Activation function	Sigmoid
Solver	LBFGS

Supplementary Figures

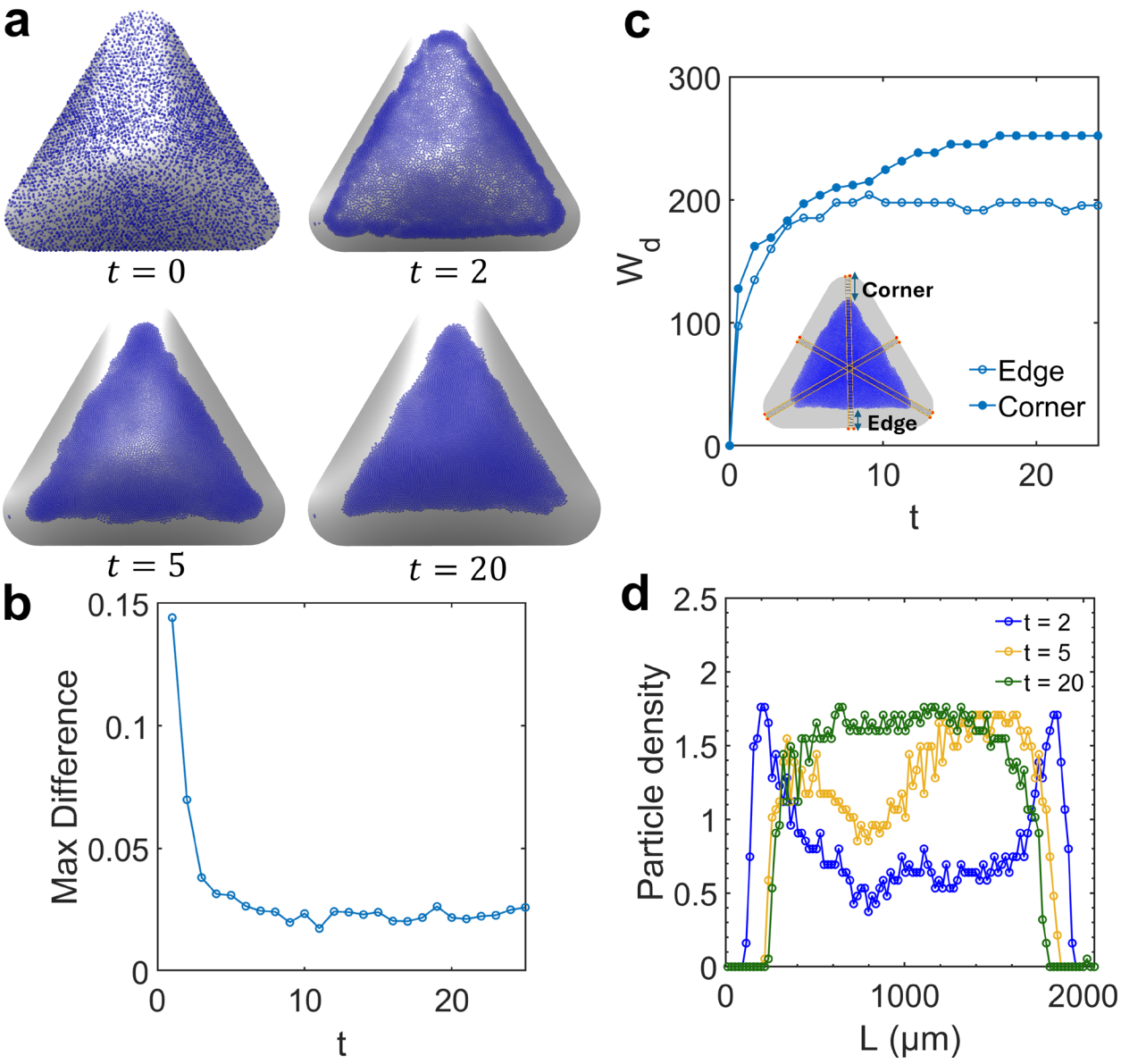

Figure S1. (a) Simulation snapshots showing the time evolution of the assembly structure, from its initial random distribution to the fully developed stage for $\sigma_p = 2 \times 10^{-3}$ C/m^2 and $\kappa = 200$ (b) Variations in particle density distributions averaged along three axes of symmetry for the triangular droplet. The maximum difference is based on a bin-by-bin comparison between consecutive time frames as a function, which monitors structural evolution toward a fully developed state. The simulation time is nondimensionalized with respect to the characteristic diffusion time $t_d = a^2/D$. (c) Time evolution of the widths of the depletion region from the edge and corner of the triangular droplet contact line (see inset). (d) Time evolution of the particle density profile averaged along three axes of symmetry for the triangular droplet.

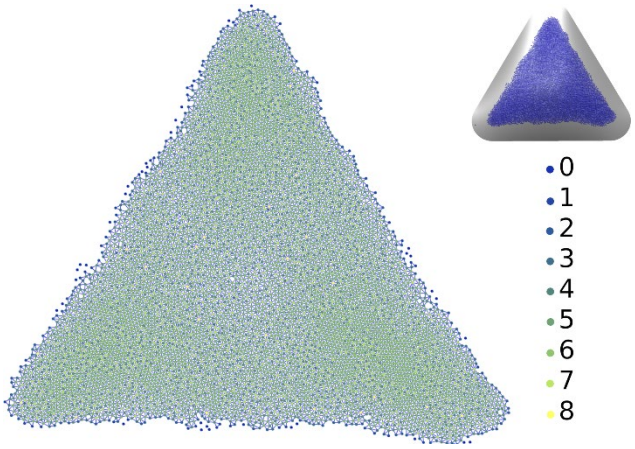

Figure S2. Heatmap of each particle coordination number calculated using Delaunay triangulation connections, which will be used in the orientational order parameter calculation for $\sigma_p = 1.6 \times 10^{-4}\ C/m^2$ and $\kappa = 180$

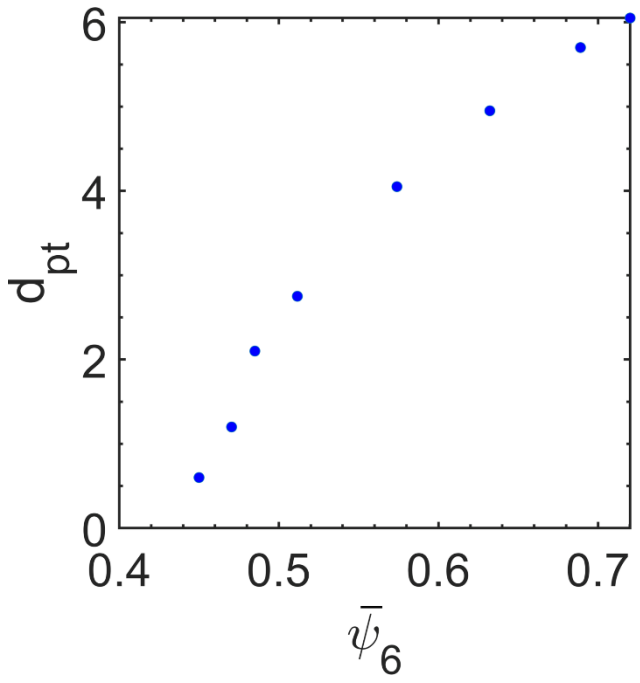

Figure S3. Correlation between the ensemble average of the sixfold orientational order parameter and the distance between the first peak and first trough in the RDF for $\kappa = 400$.

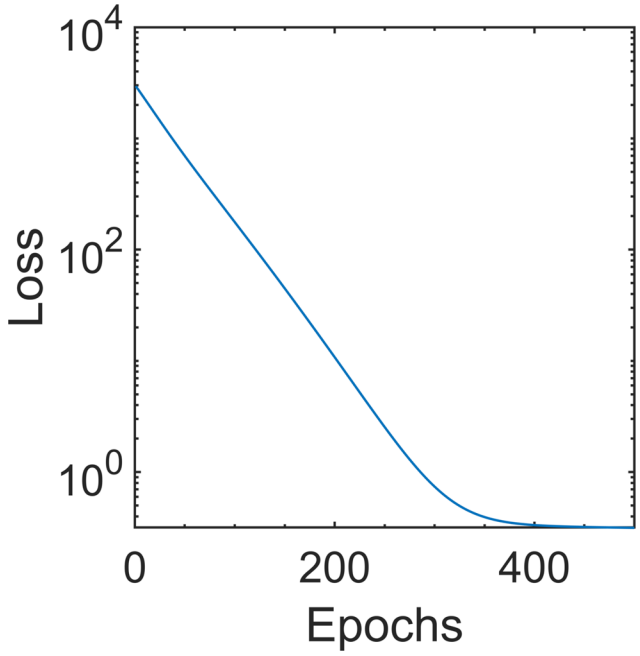

Figure S4. Artificial neural network learning curve.

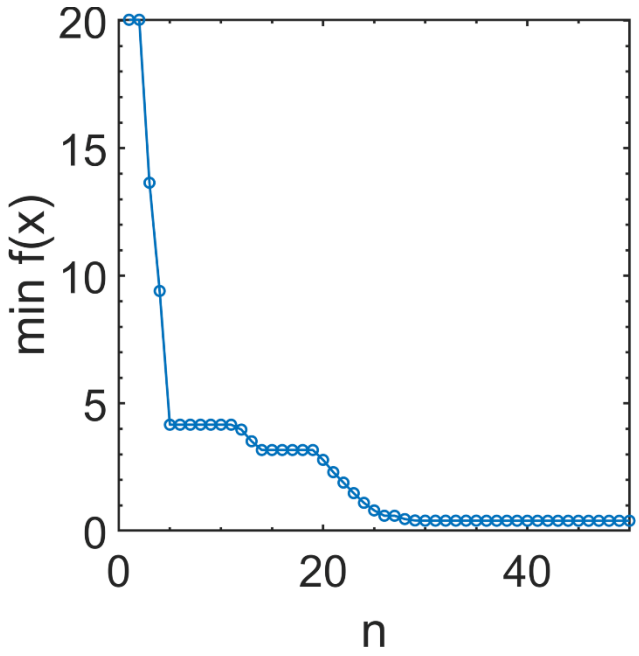

Figure S5. Bayesian optimization convergence plot.

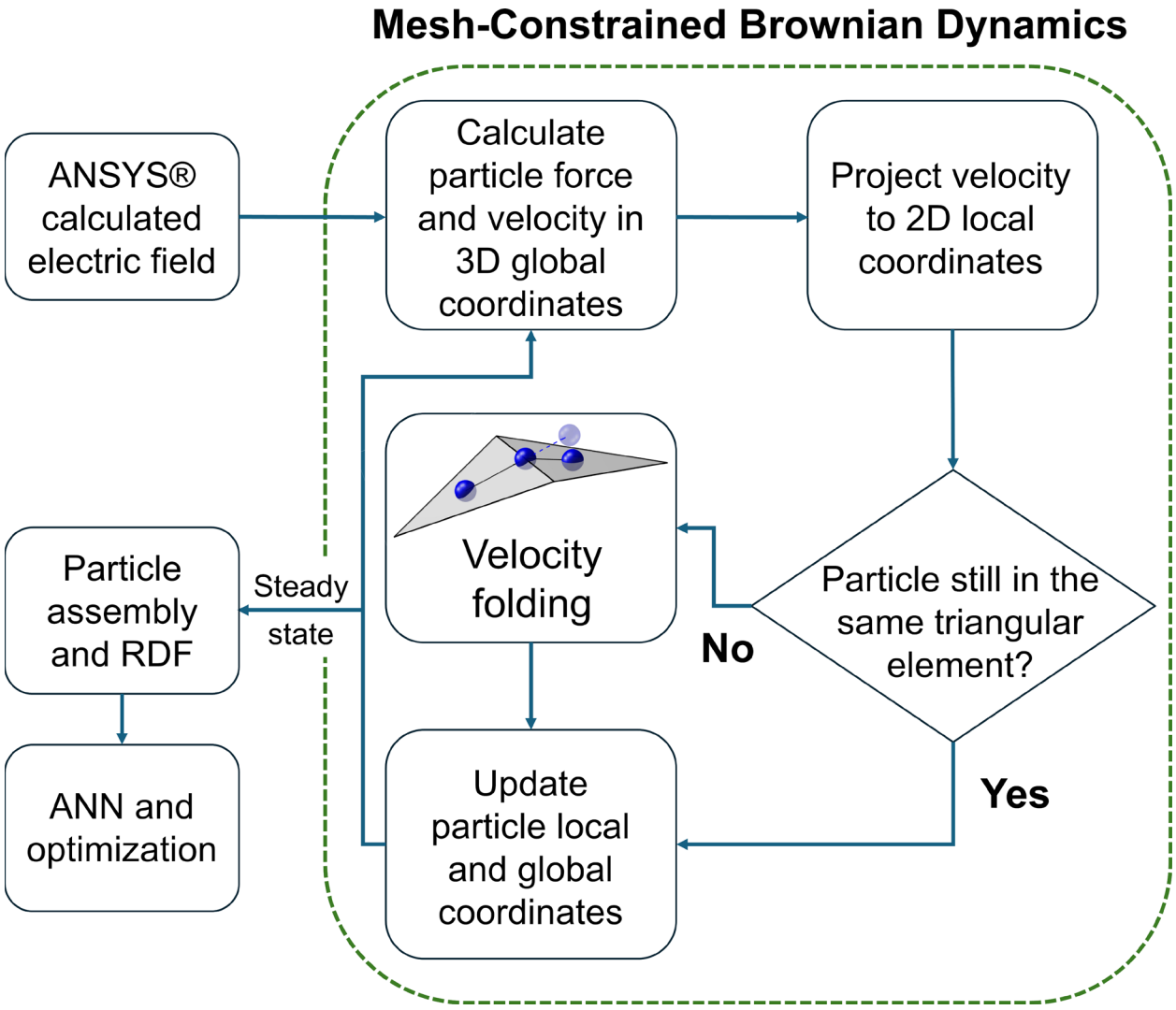

Figure S6. Flowchart of the mesh-confined two-dimensional Brownian dynamics simulation and its integration with ANSYS® electrostatic simulation, ANN surrogate training, and parameter optimization.

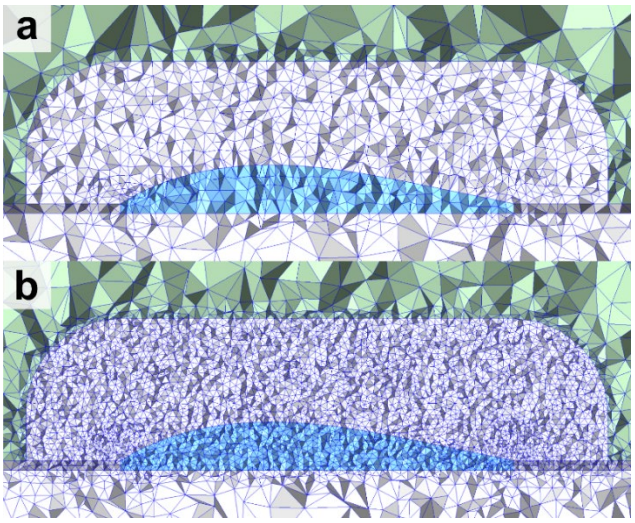

Figure S7. Mesh resolution comparison.

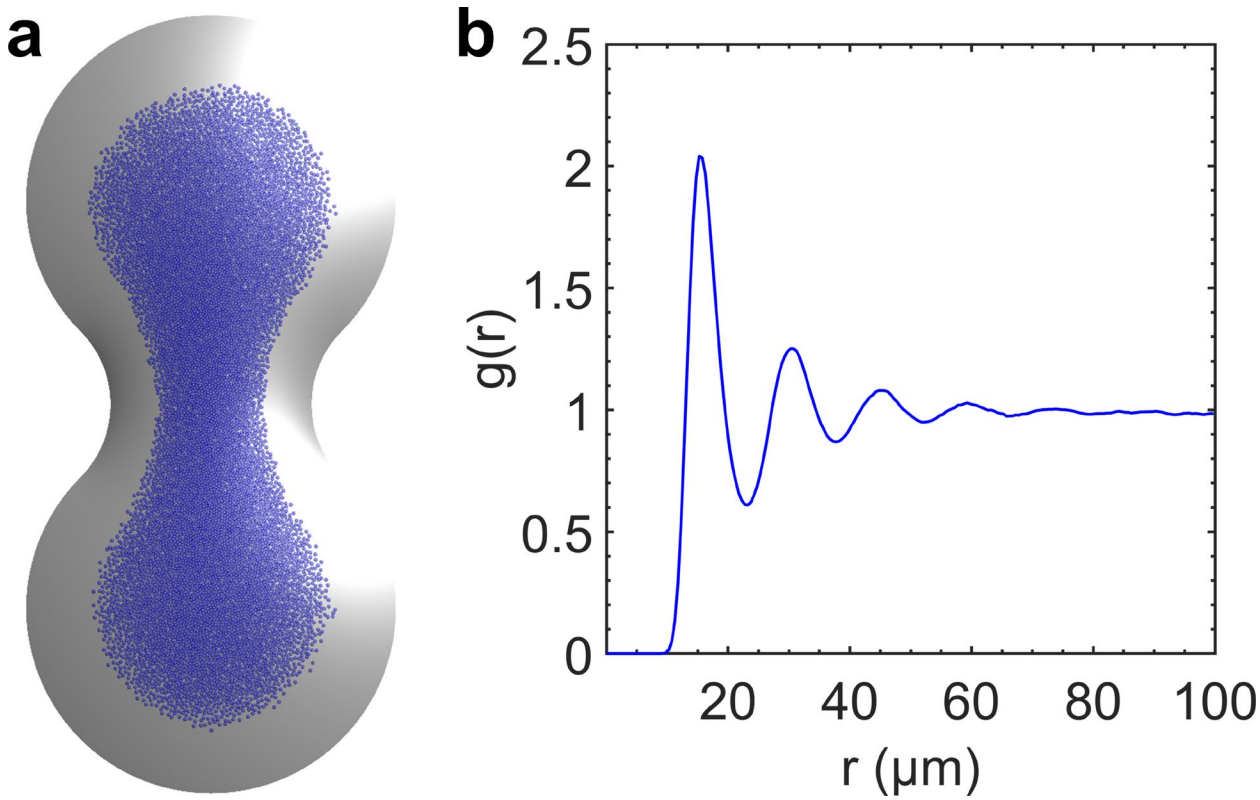

Figure S8. (a) Simulate snapshot and (b) RDF of the assembly structure on a dumbbell-shaped droplet simulated using the optimal charge densities.